https://ntrs.nasa.gov/search.jsp?R=19840002594 2020-03-21T00:46:29+00:00Z

NASA CR-168265

NASA-CR-168265
19840002594

Final Report

J.C.C. Fan

High Efficiency, Low Cost Thin GaAs Solar Cells

30 September 1982

Prepared for National Aeronautics and Space Administration
under Contract NAS C-60878-D by

Lincoln Laboratory

MASSACHUSETTS INSTITUTE OF TECHNOLOGY

LEXINGTON, MASSACHUSETTS

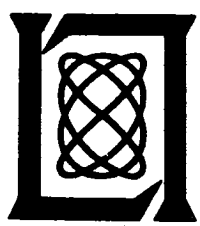

Approved for public release; distribution unlimited.

LIBRARY COPY

DEC 1984

LANGLEY RESEARCH CENTER
LIBRARY, NASA
HAMPTON, VIRGINIA

The work reported in this document was performed at Lincoln Laboratory, a center for research operated by Massachusetts Institute of Technology, with the support of National Aeronautics and Space Administration under Contract NAS C-60878-D.

The views and conclusions contained in this document are those of the contractor and should not be interpreted as necessarily representing the official policies, either expressed or implied, of the United States Government.

Technical Report Documentation Page

1. Report No.	2. Government Accession No.	3. Recipient's Catalog No.
NASA CR-168265		

4. Title and Subtitle	5. Report Date
High Efficiency, Low Cost Thin GaAs Solar Cells	30 September 1982
	6. Performing Organization Code

7. Author(s)	8. Performing Organization Report No.
John C.C. Fan	

9. Performing Organization Name and Address	10. Work Unit No.
Lincoln Laboratory, M.I.T. P.O. Box 73 Lexington, MA 02173-0073	11. Contract or Grant No. NAS C-60878-D
	13. Type of Report and Period Covered Contractor Report 1 October 1981 — 30 September 1982
12. Sponsoring Agency Name and Address National Aeronautics and Space Administration Washington, DC 20546	14. Sponsoring Agency Code

15. Supplementary Notes

16. Abstract

The objective of this program is to demonstrate the feasibility of fabricating space-resistant, high efficiency, light-weight, low-cost GaAs shallow-homojunction solar cells for space application. This program has been addressing the optimal preparation of ultrathin GaAs single-crystal layers by $AsCl_3$-GaAs-H_2 and OMCVD process. Considerable progress has been made in both areas. Detailed studies on the $AsCl_3$ process showed high-quality GaAs thin layers can be routinely grown. Lateral overgrowth of GaAs by OMCVD has also been observed, and thin GaAs films were obtained from this process.

17. Key Words		18. Distribution Statement
GaAs solar cells	space applications	Approved for public release; distribution unlimited.
CVD growth	device fabrication	

19. Security Classif. (of this report)	20. Security Classif. (of this page)	21. No. of Pages	22. Price
Unclassified	Unclassified	44	

NASA-C-168 (Rev. 10-75) *For sale by the National Technical Information Service, Springfield, Virginia 22161

N84-10662 #

ABSTRACT

The objective of this program is to demonstrate the feasibility of fabricating space-resistant, high efficiency, light-weight, low-cost GaAs shallow-homojunction solar cells for space application. This program has been addressing the optimal preparation of ultrathin GaAs single-crystal layers by $AsCl_3$-GaAs-H_2 and OMCVD process. Considerable progress has been made in both areas. Detailed studies on the $AsCl_3$ process showed high-quality GaAs thin layers can be routinely grown. Lateral overgrowth of GaAs by OMCVD, has also been observed, and thin GaAs films were obtained from this process.

CONTENTS

ACKNOWLEDGMENTS

This work was performed with the collaboration and assistance of many colleagues, especially C. O. Bozler, R. P. Gale, R. W. McClelland, and J. P. Salerno.

HIGH-EFFICIENCY, LOW-COST THIN GaAs SOLAR CELLS

The objective of this program is to develop CVD growth processes so as to produce space-resistant, high-efficiency, light-weight, low cost GaAs solar cells.

I. INTRODUCTION

We have previously reported that by using an $n^+/p/p^+$ shallow-homojunction structure, without a GaAlAs window layer, we have fabricated GaAs solar cells on single-crystal GaAs[1] and Ge[2,3] substrates with conversion efficiency as high as 21% at AM1. The 21% efficient cells on Ge, which have a GaAs epilayer only 4 μm thick, are the most efficient thin-film cells prepared to date. The Ge substrates play a passive role that permits them to be substituted for GaAs substrates without any effect on cell efficiency.

Our $n^+/p/p^+$ structures are grown by chemical vapor deposition (CVD) in an $AsCl_3$-GaAs-H_2 system with a vertical fused silica reactor.[2] Comparable cells can be obtained with either a Ga liquid source or GaAs solid source. The CVD technique potentially can be scaled up for mass production. The as-grown thicknesses of n^+, p and p^+ layers are about 0.15, 2, and 2 μm, respectively. The n^+ layer is doped with sulphur to about 5×10^{18} cm^{-3}, the p layer with zinc to about 10^{17} cm^{-3} and the p^+ layer with zinc to about 5×10^{18} cm^{-3}. We have found that cell efficiency is not very sensitive to the exact doping levels or to the thicknesses of the p and p^+ layers. However, the efficiency is sensitive to n^+ thickness.[3] Our best cells so far have n^+ layers about

500 Å thick. Although efficient cells have been fabricated with as-grown n^+ layers of this thickness, it is advantageous to grow a thicker n^+ layer and then to use an anodization and stripping process (with the front contact fingers and bars already in place) for controlled reduction of the thickness.[2] This process allows a variation in the as-grown n^+ thickness, as well as producing a larger separation between the front contacts and the junction, thus increasing the yield achieved in cell fabrication. The cells are fabricated without any vacuum processing steps, utilizing an antireflection (AR) coating about 850 Å thick prepared by anodic oxidation of the n^+ layer and electroplated Au or Sn front and back contacts during anodization.

Having succeeded in developing the highly efficient and versatile $n^+/p/p^+$ GaAs shallow-homojunction structure we have investigated processes to greatly reduce the weight of such cells without a significant reduction in cell efficiency. To retain high efficiency, we believe that the cells should utilize thin GaAs layers that are single crystalline. A novel growth process, CLEFT process, was developed[4] to produce single crystalline GaAs layers from reusable substrates. Since many films can be obtained from one substrate, this process should permit a marked reduction in material usage and cost; since single-crystal films are used, cell efficiencies should remain high; since the films are only a few microns thick, such cells can have very high power-to-weight ratios.

The CLEFT process is a peeled-film technique. The basic idea of peeled-film technology is to grow a thin single-crystal epilayer on a

single-crystal mold, to separate the epilayer from the mold, and then to use the mold again (see Fig. 1).

The key element of the CLEFT process is the use of lateral epitaxial growth performed in a CVD reactor. Our experiments have shown that if a mask with appropriately spaced stripe openings is deposited on a (110) GaAs substrate, the epitaxial growth initiated on the GaAs surface exposed through the openings will be followed by lateral growth over the mask eventually producing a continuous single-crystal film that can be grown to any desired thickness. The upper surface of the film is then bonded to a secondary substrate of some other material. If there is poor adhesion between the mask material and the GaAs, the film will be strongly attached to the GaAs substrate only at the stripe openings. Since a weak plane has been created by the mask and because the (110) plane is the principal cleavage plane of GaAs, the film can be cleaved from the GaAs substrate without significant degredation of either (Fig. 2). We have found that carbonized photoresist is a suitable mask material, since it has the necessary poor adhesion to GaAs and is chemically inert under the conditions that we employ for growth. Other mask configurations have also bee used, including SiO_2-coated carbonized photoresist masks which provide somewhat better surface morphology for GaAs CLEFT films.

In this report we will first describe the the lateral growth process in the $AsCl_3$-GaAs-H_2 system. We will then present some results obtained in the OMCVD system.

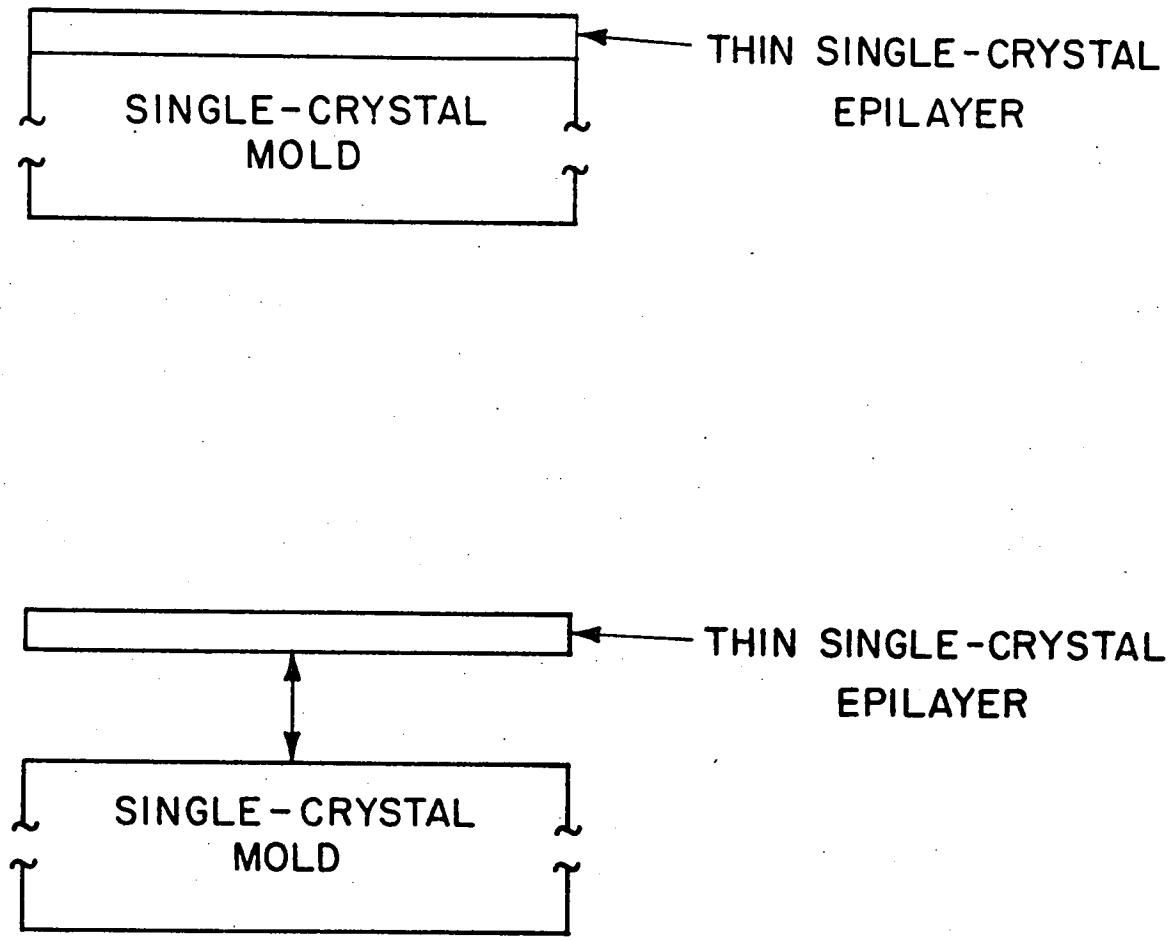

Fig. 1 Schematic diagram showing the peeled-film technology.

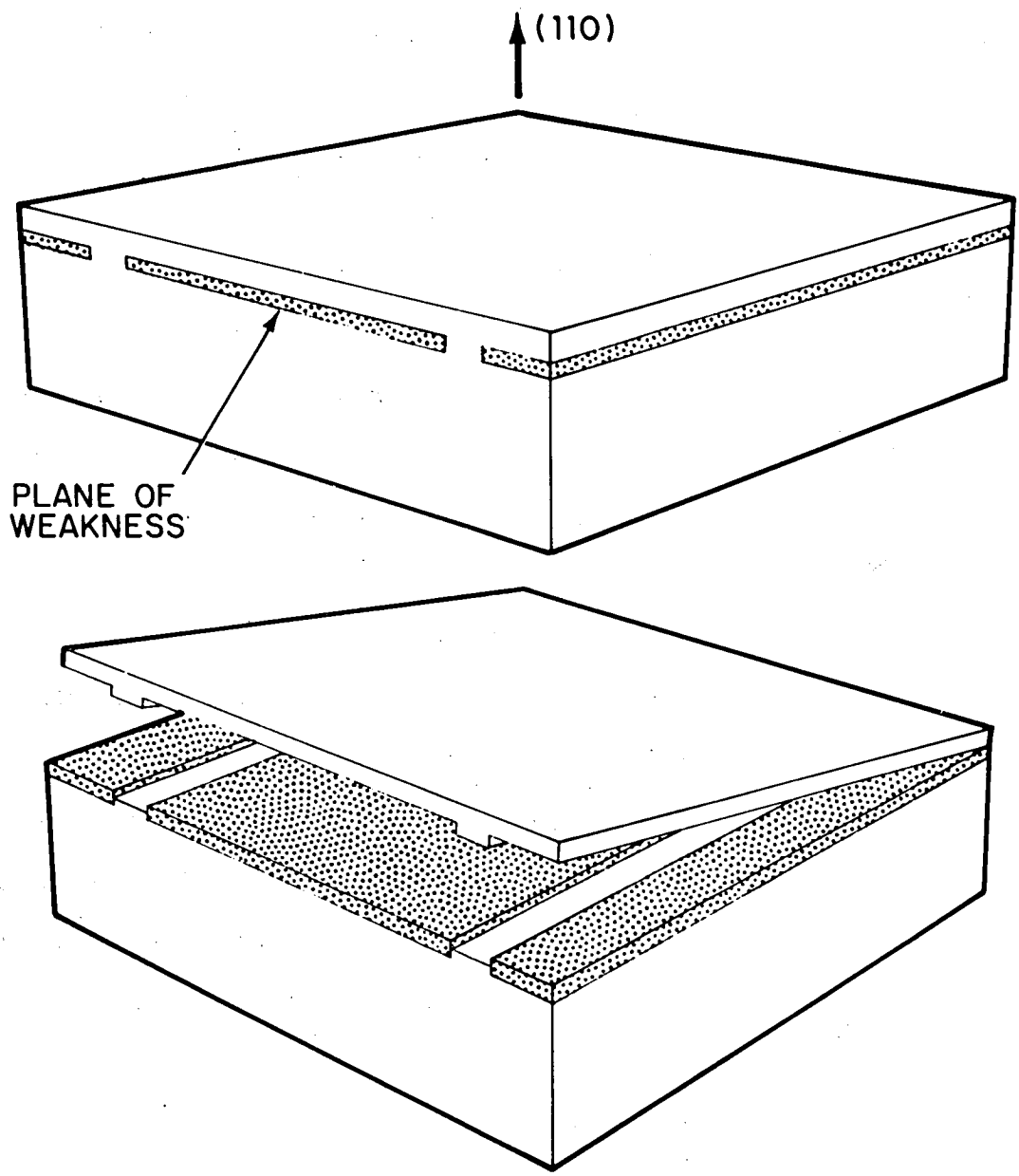

Fig. 2 Schematic diagrams of the CLEFT process, illustrating the separation of an epilayer from its substrate.

II. As_2Cl_3-GaAs-H_2 SYSTEM

The growth system, which has been described before,[2] used the $AsCl_3$-GaAs-H_2 process. The first experiments with the CLEFT process used a liquid Ga source, but all of the experiments described below have used a GaAs source, which permits more convenient system operation. We believe it is the Cl used for transport of the Ga in the $AsCl_3$ process which is a key requirement for achieving the lateral growth over distances of many micrometers in this growth process. The Cl or HCl in the reactor atmosphere causes the Ga to have a low sticking coefficient and therefore a low nucleation rate on the growth mask, so that crystal growth occurs only on the GaAs. Any of the other halogens and possibly oxygen could function in a similar way to provide selective growth.

Because of the large number of significant variables, it is difficult to quantify lateral growth at this early stage of development. The parameters that have been found to have the greatest effect on lateral growth are orientation of the single-crystal substrate, orientation of the slit openings with respect to the substrate, substrate temperature during growth, and $AsCl_3$ vapor pressure. We will give a qualitative description of the effects of these parameters.

A. Substrate Crystal Orientation

Since the CLEFT process requires cleaving of the film parallel to the substrate surface, this surface should be an easy cleavage plane. For GaAs the (110) planes are the principal cleavage planes. Previous work on vertical growth rate as a function of substrate orientation[6-9] has shown that this rate

has minima for the (110), (100),and (111) planes. Under certain conditions the (110) planes have a smaller growth rate than any others. This is advantageous for the CLEFT processes since vertical growth on a (110) plane will be smaller than lateral growth in almost all the other directions, tending to maximize lateral to vertical growth rate ratio. Misorientation of the growth surface by a little as 1 or 2 degrees away from the (110) plane rapidly increases the vertical growth rate and therefore signifcantly reduces this ratio. Consequently the misorientation should not exceed a few tenths of a degree.

B. Slit Opening Direction

The direction of the slit openings in the growth mask with respect to the crystal lattice of the substrate has a very strong effect on lateral growth. In order to study this effect we have used a special growth mask (Fig. 3). The mask contains a circular array of radial parallel pairs of slit openings indexed at 1 degree intervals over a full 360°. This spoke pattern allows us to observe how the two growth fronts from each pair of adjacent openings merge as a function of angle, and enables us to choose an optimum slit opening orientation for growth of CLEFT films.

Since overgrowth has been found to be the same over SiO_2 as on the composite mask used in the CLEFT process, for testing purposes a single-level SiO_2 mask is used. A masked substrate is placed in the epitaxial system and growth is allowed to proceed until the film is 2 to 4 μm. Figure 4 is an optical micrograph showing the result of one such test. The amount of lateral growth varies periodically with the angle of the openings in the spoke

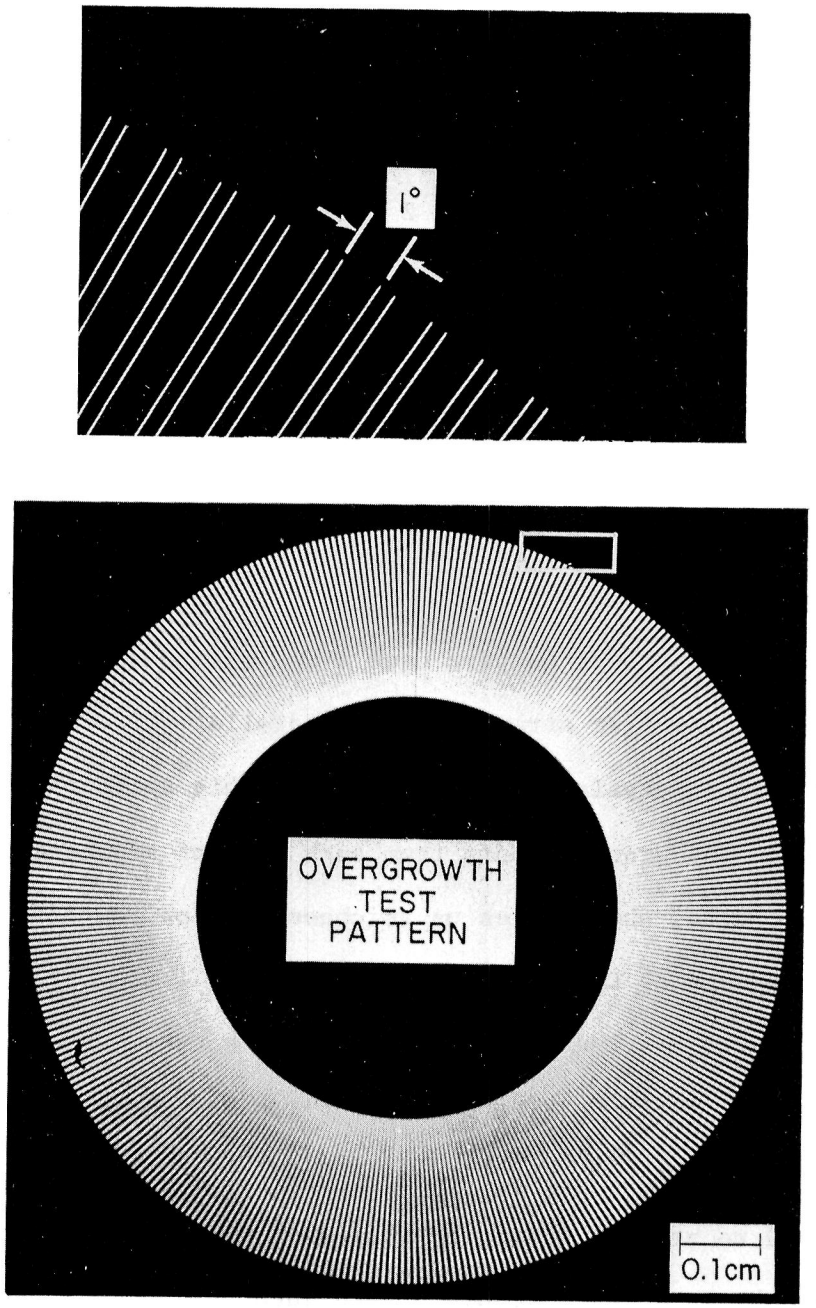

Fig. 3 Optical micrograph of a test pattern having an array of pairs of radial slit openings in one degree increments.

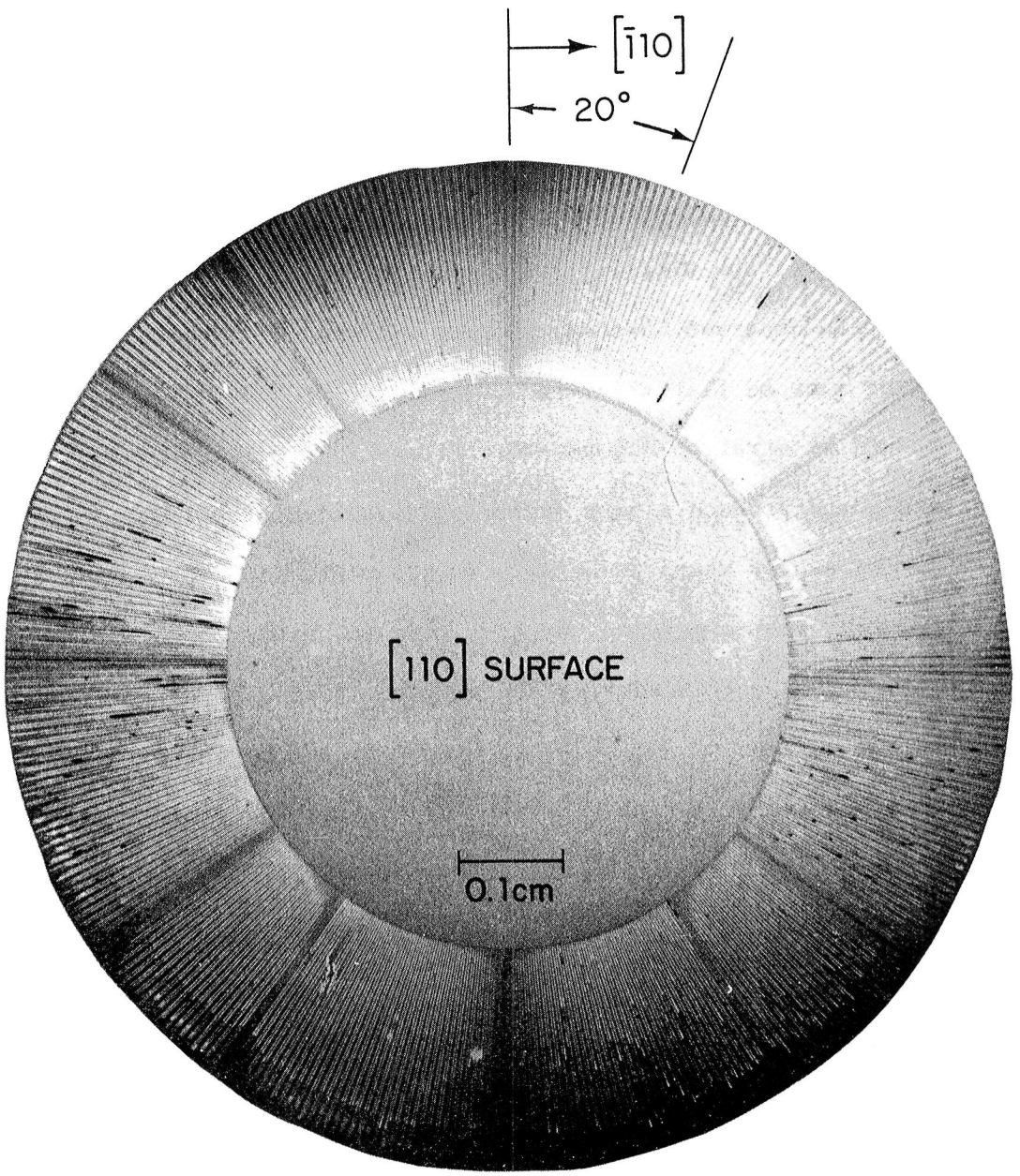

Fig. 4 Optical micrograph of selective epitaxial overgrowth over a SiO_2 mask with the test pattern shown in Fig. 3.

pattern. The minimum growth occurs at angles corresponding to the (110), (100), and (111)B planes.

To determine the optimum slit direction from a test like the one of Fig. 4, four main criteria are used. First, there must be sufficient lateral growth to allow the growths from the two openings to join. This will of course depend on the growth time, the lateral to vertical growth rate ratio and the spacing of the slits. Lateral to vertical growth rate ratios as large as 70 have been observed. Second, the top surface of the growth from each opening must be flat and without striations. Third, the lateral growth fronts should be straight and smooth. Fronts with serrations will join nonuniformly and produce a very disturbed crystalline region. Fourth, there should not be a step where the growth fronts join, since otherwise the CLEFT film will develop a corrugated surface.

Figure 5 is a magnified view showing the morphology of the lateral growth in one region of Fig. 4. In order to precisely define the direction of the slit openings relative to the substrate crystal we have chosen the (110) plane as the reference, since this is the only cleavage plane perpendicular to the surface of a (110) wafer. For the pair of slits at 20° in Fig. 5, the first three criteria described above are satisfied; the fourth criterion cannot be checked because the growth fronts have not joined. For the same angle region as in Fig. 5, an experiment was done in which the growth time as long enough for the growth fronts from each pair of slits to join. For the pair of slits at 20° the intersection between the fronts is very smooth, satisfying the

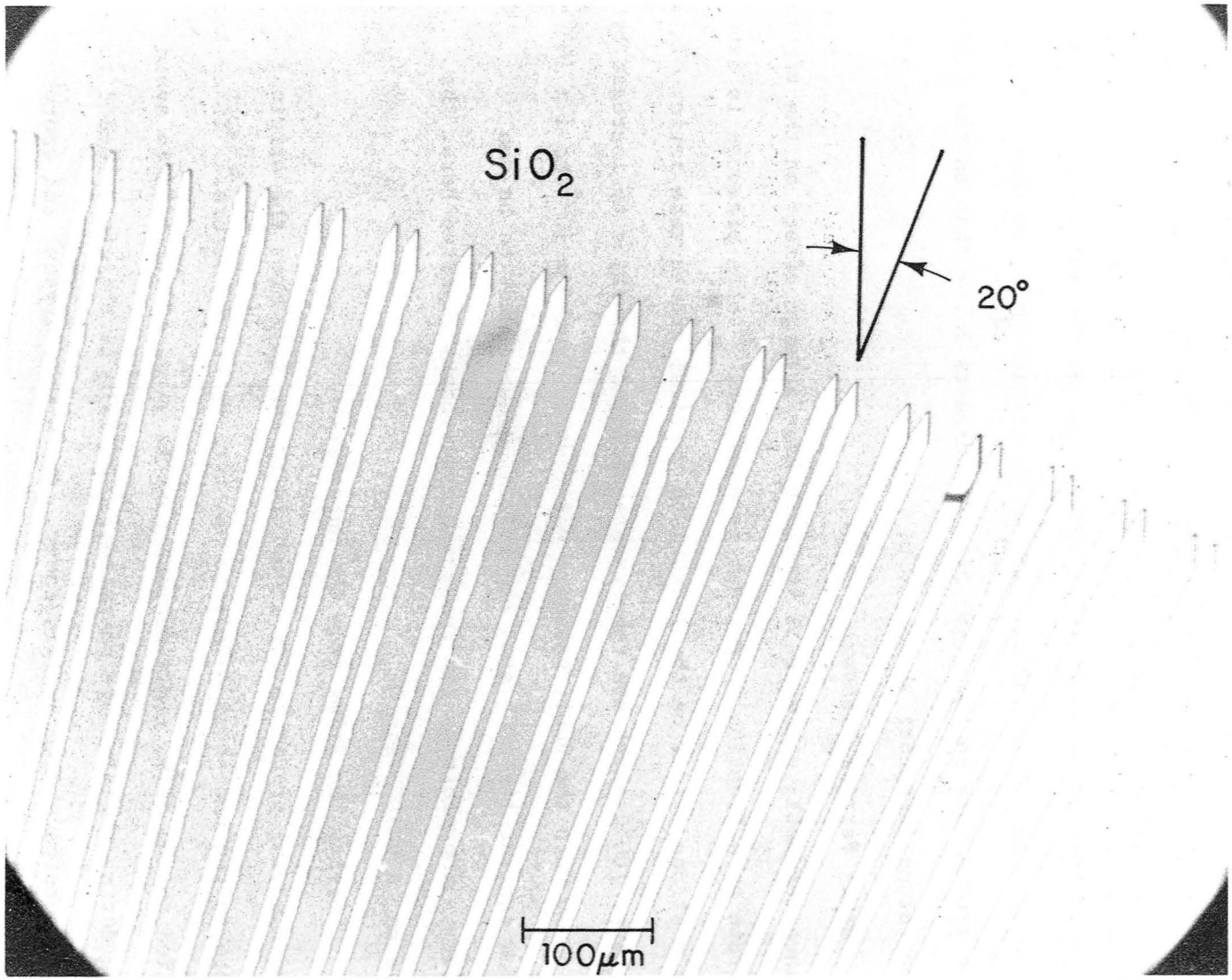

Fig. 5 Optical micrograph of an enlarged view of a region of the micrograph in Fig. 2 showing the lateral growth where the slit openings form angles of about 20° with the (110) direction.

fourth criterion. Therefore, in the remaining experiments reported here, the angle chosen for the slits was 20°.

C. Substrate Temperature

The substrate temperature used for the test wafer shown in Fig. 4 was 720°C. In experiments at several temperatures we have found that the lateral to vertical growth rate ratio tends to increase as the substrate temperature is increased from 700 to 750°C. This is consistent with the observcation[9] that the growth rate on the (110) planes decreases below that on the (100) as the temperature increases above 700°C.

D. $AsCl_3$ Partial Pressure

Since the $AsCl_3$ pressure is known to have a large effect on the vertical growth rate as a function of crystal orientation,[6-9] this pressure is expected to have a strong effect on the lateral to vertical growth rate ratio. In a few tests at 700°C substrate temperature we found the ratio to increase by a factor of 10 when the $AsCl_3$ pressure was reduced from 4×10^{-3} to 1×10^{-3} atm. However, at 1×10^{-3} atm, the lateral growth tends to be too nonuniform. Therefore in the remaining experiments reported here, the pressure as $\sim 4 \times 10^{-3}$ atm.

E. Cleaving the Films from the Substrate

The cleaving procedure for transferring the film from the original substrate to the amorphous substrate has been described before.[4] Since force is applied to the film, rigid support must be given to the film to avoid cracking during the cleavage operation. The film is therefore bonded to the amorphous substrate with a rigid epoxy. The single-crystal and amorphous

substrates are bonded with wax to 5-mm-thick glass plates to minimize flexing during the cleaving operation. This rigidity appears to provide the proper dynamics for the very rapid motion of the cleaving front passing between the film and the single-crystal substrate. Figure 6 is an optical micrograph showing the top of the single-crystal substrate and the bottom of the film after cleaving. The ribs left behind on the substrate are about 300 Å high. The total rib height is equal to the thickness of the growth mask, which consists of 700 Å carbon and 1000 Å SiO_2. The cleaved surfaces of the ribs are extermely smooth, indicating the uniformity of the cleaving process. The dashed lines seen between the cleaved ribs on the bottom of the film are depressions formed at the intersections between growth fronts.

F. Crystal Quality

A number of properties are important in determining whether a CLEFT film is useful for semiconductor device applications. The dislocation count is of interest because dislocations are often detrimental to p-n junctions, Schottky barriers, and carrier lifetimes. The concentrations of unintentional impurities are important because they may reduce lifetime and carrier mobility and because they restrict the useful range of dopant impurity concentrations that can be used in device fabrication. The uniformity with which dopants can be incorporated is also important for the design and reproducible construction of devices.

Mobility measurements have been made on several CLEFT films. A value of 20000 $cm^2\ V^{-1}S^{-1}$ at 77 K has been obtained for a S-doped, n-type film with a carrier concentration of $1 \times 10^{16}\ cm^{-3}$. This is comparable to values obtained

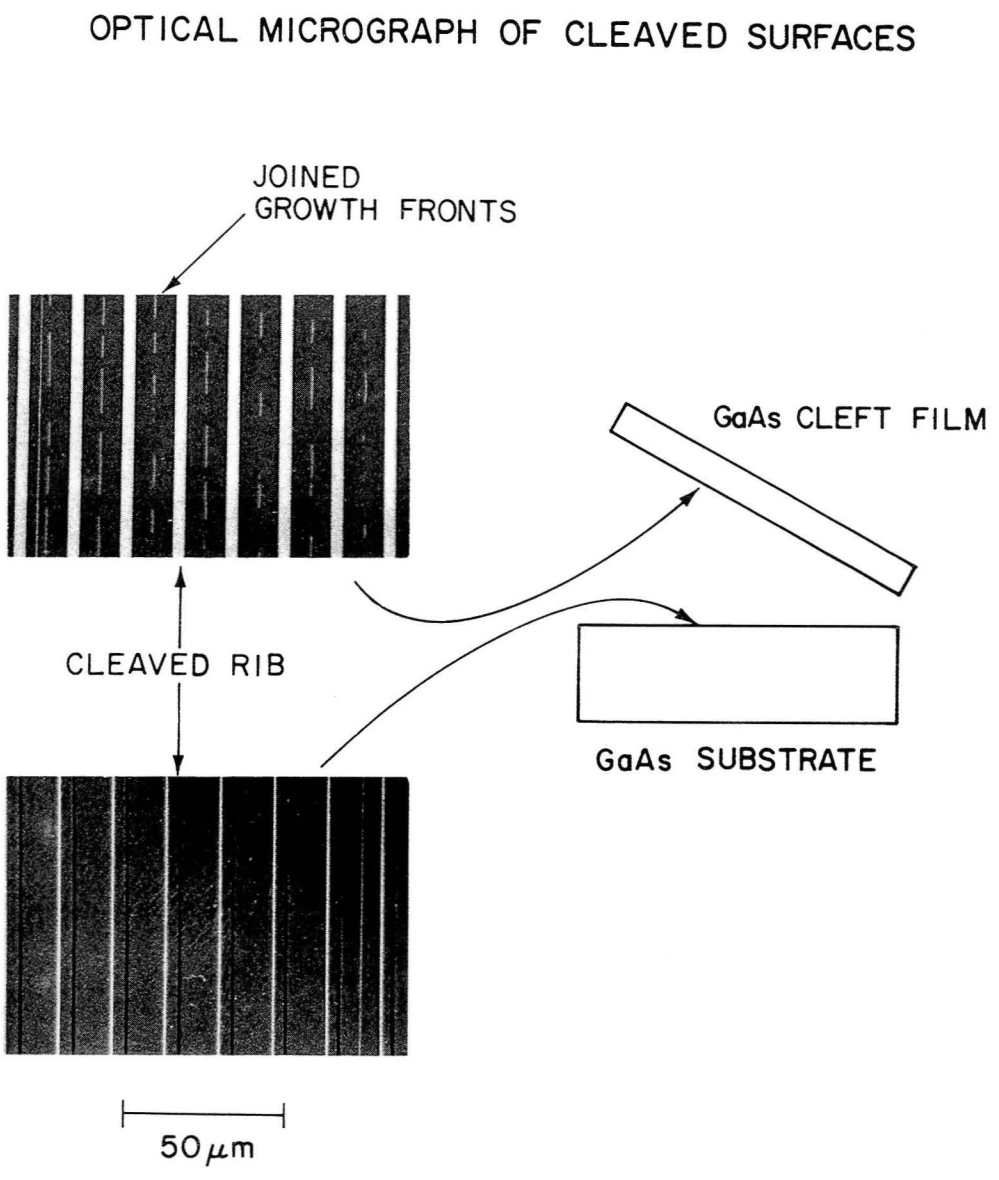

Fig. 6 Optical micrographs of the cleaved surfaces of a CLEFT film and its single-crystal substrate. The dashed lines between the ribs on the bottom of the film are long narrow depressions in the surface due to voids.

for conventional films having the same carrier concentration, indicating that the residual impurity concentration in the CLEFT films is low enough for most device most device applications. Solar cells with efficiencies as high as 17% at AM1 have been made from CLEFT films.[10] The high efficiency indicates that the films have carrier lifetimes comparable to conventional epitaxial films. Although the electrical properties already indicate that the films are useful for device applications, we have also made some studies of dislocation density and carrier concentration uniformity.

There are several potential sources of dislocations in a CLEFT film. These include threading of dislocations from the substrate crystal though the slit openings in to the film, misalignment along the intersections between the lateral growths from neighboring slits, interactions between the GaAs and the growth mask, and stress generated during the cleaving process.

The dislocation density was investigated by TEM, dislocation etching and SCM. In the TEM studies we inspected many samples under a number of diffraction conditions but in total only two defects were found, both of which were dislocations located at a significant distance from the intersections between growth fronts (see Fig. 7). Although the total area examined by TEM was relatively small, it is encouraging that no defects associated with the joining of the growth fronts were found. The very small number of defects detected by TEM indicates that the dislocation density is less than 10^5 cm^{-2}.

The usual dislocation etch[11] did not reveal any dislocations. This is not surprising, since an etch depth of 60 μm is required for a reliable count,

110074-R

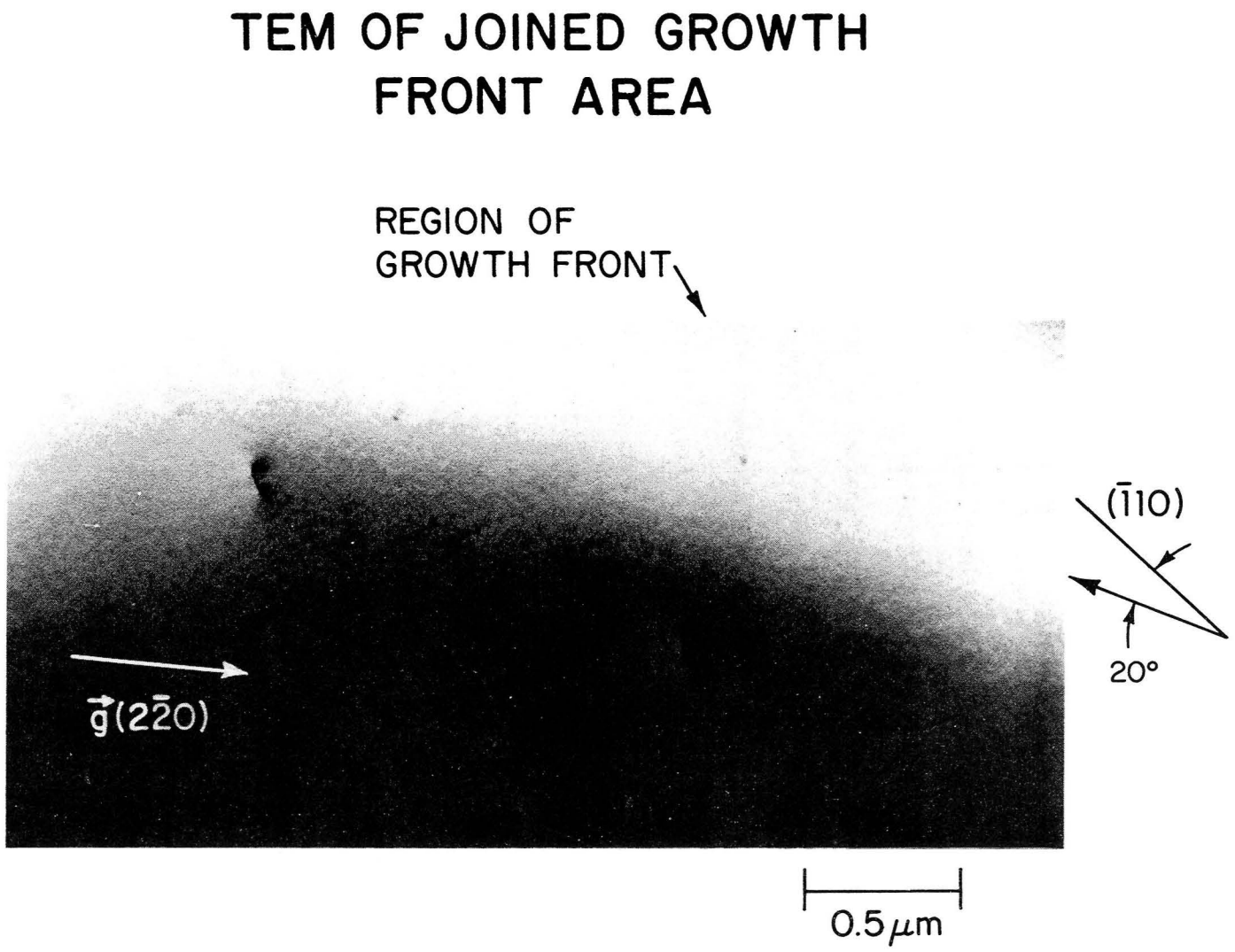

Fig. 7 TEM micrograph of a CLEFT film, showing some dislocations.

but the films were only 5-10 μm thick. The dislocation etch did reveal carrier concentration inhomogeneities as described below.

Nonradiative recombination centers, such as dislocation, or precipitates, or carrier concentration differences, can be detected by SCM to depths of several micrometers. Figure 8 is a typical SCM micrograph of a CLEFT film, which does not reveal any defects. Micrographs obtained for many films indicate that the dislocation densities are 10^3 cm^{-2} or lower, significantly less than the values of about 10^4 cm^{-2} found for the GaAs substrate. The alternating dark and light bands are due to carrier concentration variations resulting from differences between the orientations of the fronts growing in the two opposite directions from the stripe openings, as will be discussed in the next section.

The CLEFT films were intentionally doped with sulfur to a level of about 1×10^{16} cm^{-3}. To investigate the impurity distribution in a film, a ferrocyanide solution was used to stain a cleaved cross section of the film while it was still attached to the single-crystal substrate. Figure 9(a) is an optical micrograph of a stained cross section of a CLEFT film and its substrate, and Fig. 9(b) is a schematic diagram of the stain lines. Each of these lines shows the location of the boundary between regions with different carrier concentrations. The two black areas in the diagram represent voids formed at the intersections between growth fronts which create the depressions shown in Fig. 6. The reason for the carrier concentration variations is illustrated in Fig. 10 which schematically shows the cross-sectional outline of the lateral overgrowth at successive times. The overgrowth is bounded by

109931-N

SCANNING CATHODOLUMINESCE OF SURFACE SIDE

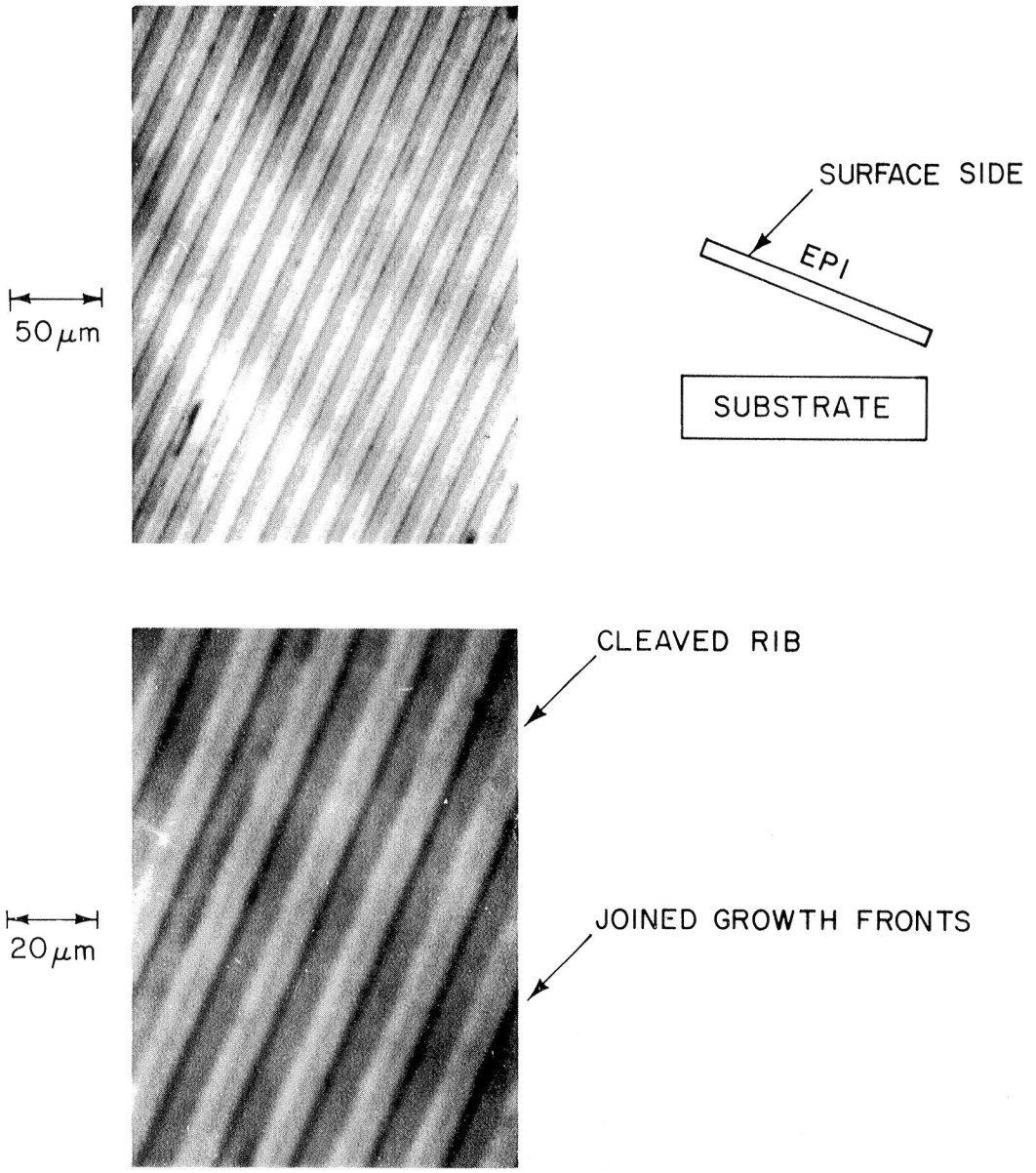

Fig. 8 Scanning cathodoluminescence micrograph of the cleaved side of a CLEFT film. The stripes are due to the nonuniformity of the carrier concentration, the dark splotch in the lower right corner is due to surface contamination.

109932-N

OPTICAL MICROGRAPH OF STAINED CROSS SECTION

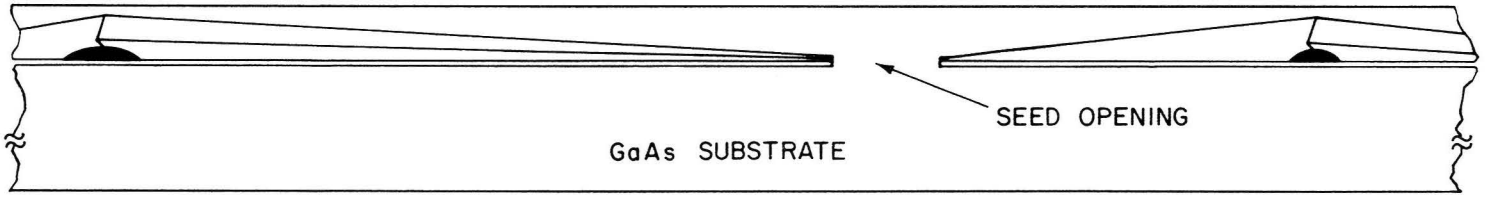

Fig. 9 (a) Optical micrograph of stained cross section of a 6-μm-thick CLEFT film on its single-crystal substrate. (b) Schematic diagram showing the stain lines, the growth mask, mask openings and voids.

109790-N

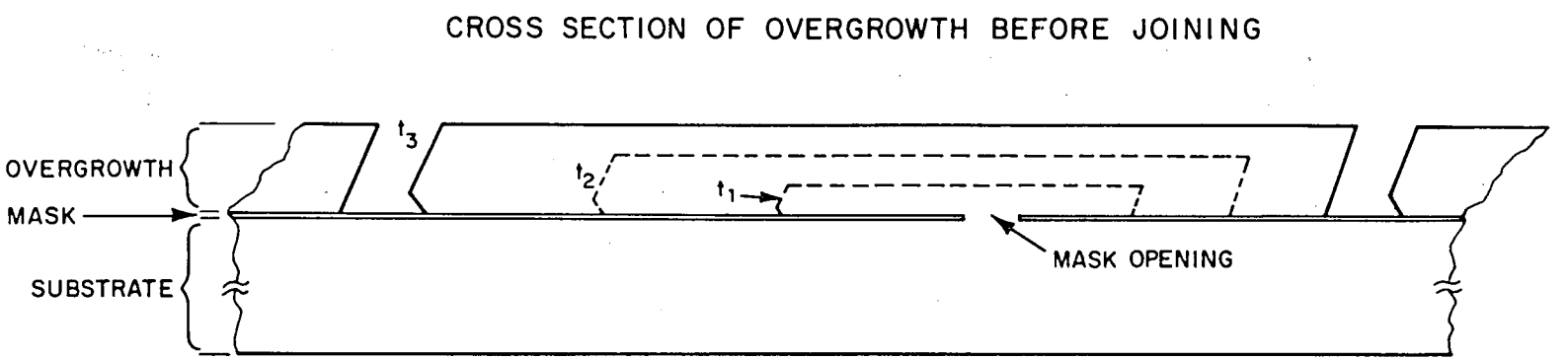

Fig. 10 A Schematic drawing of the crystal cross-section of successive times during its growth showing how the stain lines and voids of Fig. 7 are formed. Growth occurs on four different planes, which have different dopant incorporation rates.

four growth planes with different rates. During growth the rate of sulfur incorporation differs from plane to plane, leading to the formation of the regions with different carrier concentration. As the overgrowth proceeds the intersections between planes trace out the dashed lines which are the boundaries between regions of differing carrier concentration. After the overgrown film becomes continuous there is only one growth plane, parallel to the substrate surface, so that further growth yields a uniform concentration.

In some devices, such as solar cells, inhomogeneities in carrier concentration should not have a major effect provided they are not located in the active region. The thickness of the inhomogeneous region can be minimized by adjusting the lateral to vertical growth rate ratio and the spacing of the slit openings in the mask. For other devices it would be desirable for the concentration to be uniform. This might be accomplished by using a dopant whose distribution coefficient is less orientation dependent than that of sulfur or by finding growth conditions where the sulfur incorporation rate is not so strongly dependent on orientation.

G. Solar Cells

Figure 11 is a schematic diagram of the cross section of a CLEFT solar cell. The structure of this cell is unique in several respects. The entire thickness of GaAs is less than 10 μm, compared with ~300 μm for our conventional cells. The glass substrate has a dual role, since it both supports the film and serves as the cover glass for the cell. This illustrates that for some applications the amorphous substrate can be more

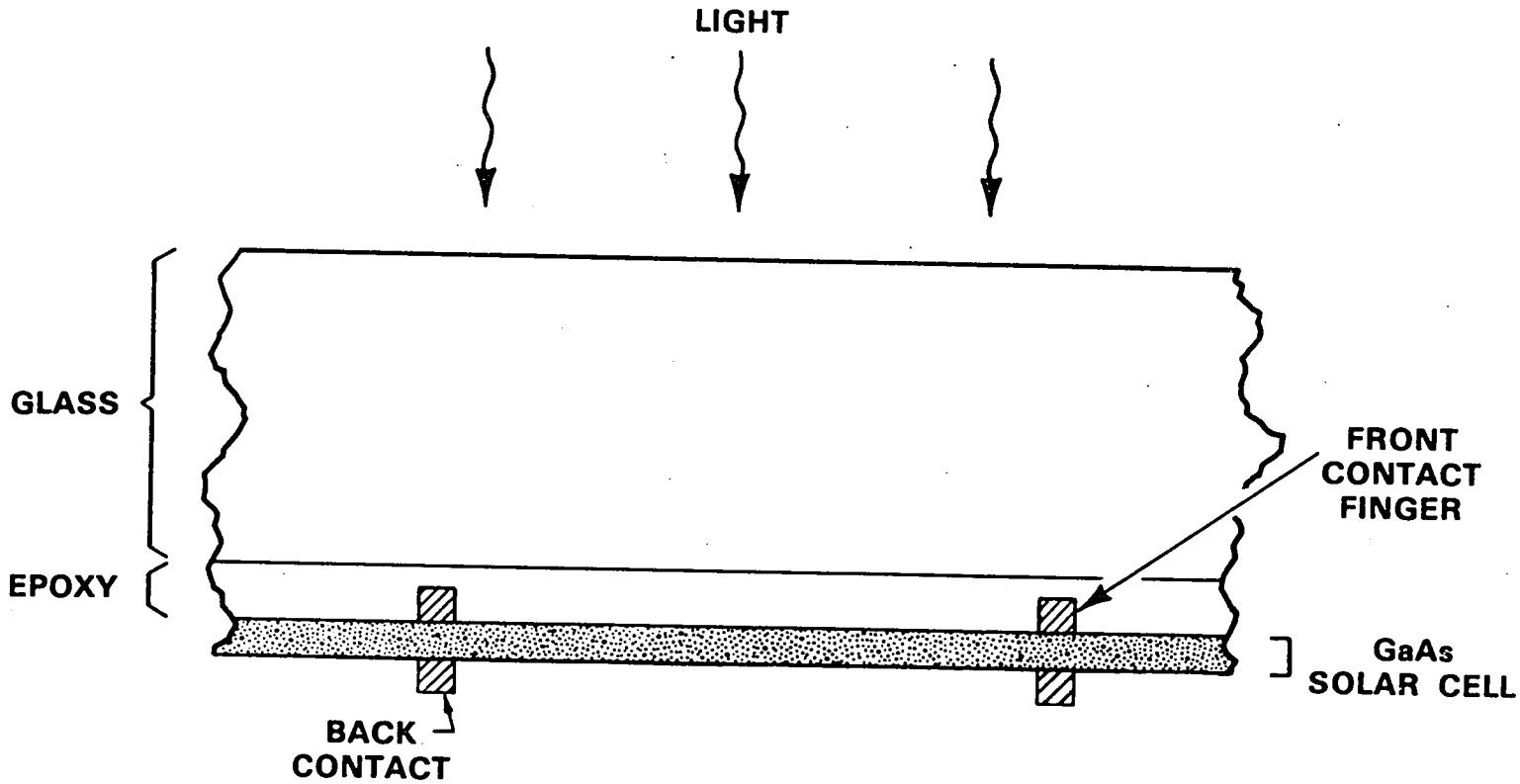

Fig. 11 Cross-sectional view of a completed CLEFT cell, in which the glass substrate serves as the protective cover glass. Notice the open grid configuration at the bottom of the cell.

useful than a single-crystal substrate. In addition the glass substrate is much less expensive than the original GaAs substrate. Another advantageous aspect of the structure is that there are metal contacts on both sides of the GaAs film. The two-sided metallization would be especially useful for devices where the current flow is perpendicular to the surface, e.g., in tandem solar cells.

A number of CLEFT cells have been fabricated with efficiencies ranging from 14 to 17% at AM1. The thinnest cell made so far has GaAs layers only 5.5 μm thick. This cell has a conversion efficiency of 17.3% at AM1, and 14.3% at AM0. This cell has a cell area of 0.51 cm^{-2}, with Au contacts on the front and back of the cell. The front and back contacts are both opened, and spaced to 50 mil apart. The contact fingers are about 1/2 mil wide and about 1 μm thick. The open-grid structure in the back contact allows for the lighter weight, and is essential for tandem-cell structure.

III. OMCVD SYSTEM

As discussed in the previous sections, lateral growths were normally carried out by the $AsCl_3$-GaAs-H_2 technique which used HCl in the deposition process. Utilization of OMCVD for lateral overgrowth would offer two important advantages over the halide technique. First, since OMCVD does not employ HCl, it can be used with reactant or substrates that are adversely affected by reaction with HCl. For example, materials containing Al can readily be grown by OMCVD. Second, OMCVD permits convenient deposition of layers of ternary and quaternary alloys. However,there has been some doubt

whether OMCVD, as a highly nonequilibrium process, would exhibit the strong orientation dependence of growth rate that is required for significant lateral growth. Lateral epitaxial overgrowth by OMCVD was observed.[13] To demonstrate the applicability of this technique to the CLEFT process[4,5] we have grown a continuous GaAs layer over a patterned mask on a GaAs substrate and removed the layer from the substrate by cleaving.

Our primary motivation for investigating overgrowth by OMCVD is to develop a method for fabricating ultrathin, wide-band-gap photovoltaic cells by the CLEFT process. Bonding one or two such cells to a lower band-gap cell would yield a cascade structure that could exhibit conversion efficiencies up to 30% at AM1[12] while avoiding the problems of lattice and photocurrent matching inherent in monolithic cascade cell designs. The OMCVD process, which has been used to prepare conventional epilayers for GaAlAs solar cells,[14] is well suited for precise control of composition and doping in multicomponent structures.

The OMCVD system used for growth of GaAs is typical of reactors employing rf induction heating.[15] The quartz reactor tube is mounted horizontally, and the upper surface of the graphite susceptor is parallel to the reactor and gas flow. Growth temperature is monitored by a thermocouple inserted into one end of the susceptor. Trimethylgallium (TMGa) is maintained at constant temperature in a bubbler with hydrogen used as the carrier gas. The arsenic source is a 5% mixture of arsine in hydrogen. The streams of each source and carrier gas, which are electronically controlled, are combined in a manifold

before entering the reactor at atmospheric pressure (see reference 16). All layers in this study were heavily doped p type with a mixture of dimethylzinc in hydrogen.

The substrates were p-type (5×10^{18} cm^{-3}) GaAs (110) wafers. After being polished, cleaned and etched, each had 1000 Å of CVD SiO_2 deposited on its front surface. A pattern of narrow stripes exposing the substrate was then opened in the oxide by standard photolithographic techniques. Lateral overgrowth was investigated for growth temperatures between 680 and 850°C and for growth times between 15 and 120 min. The TMGa mole fraction was normally 1.2×10^{-4}, which gave an average vertical growth rate of 3 μm/h, and the AsH_3 mole fraction was normally 3.6×10^{-3}.

To investigate the dependence of overgrowth on the orientation of the stripe openings in the SiO_2 with respect to the substrate, we used an oxide test pattern previously employed for $AsCl_3$-GaAs-H_2 overgrowth studies.[5] This pattern is formed by etching 360 pairs of parallel stripe openings 3 μm wide and 20 μm apart, indexed at 1° intervals, that radiate from a central circle where the SiO_2 remains intact (see Fig. 3). Figure 12(a) is a photograph of the surface of a patterned sample after a GaAs growth run at 750°C. The lateral growth is seen to be strongly orientation dependent, exhibiting the double two-fold symmetry of the (110) plane. The light areas in Fig. 12(a) are smooth GaAs surfaces, the gray areas are SiO_2, and the fine dark spots in the gray areas are polycrystalline GaAs nucleated directly on the SiO_2. The light squares in the central circle and at the pattern perimeter are GaAs deposits formed by vertical epitaxial growth on exposed square areas of the

substrate. The pairs of stripe openings corresponding to the 12 low-index directions for lateral growth are indicated in Fig. 12(a) by symbols drawn in the central circle designating the [001], [1$\bar{1}$0], [1$\bar{1}$1], [$\bar{1}\bar{1}$1], [1$\bar{1}$2], and [$\bar{1}\bar{1}$2] orientations.

To determine the quantitative dependence of lateral growth on orientation, we have measured the total width of the GaAs layer originating within each stripe opening. Figure 12(b) is a polar plot showing these widths (which include the 3-μm width of the opening) for the sample of Fig. 12(a) as a function of the angular positions of the openings. Overgrowth minima occur for openings corresponding to the 12 low-index growth directions indicated in Fig. 12(a), with the least overgrowth taking place for the two [1$\bar{1}$0] openings, (i.e., the openings that have their long axis normal to the [1$\bar{1}$0] direction). Minima also occur for these 12 orientations in overgrowth on (110) substrates by the $AsCl_3$-GaAs-H_2 process.[5] For the openings close to the two [001] openings, the surface morphology is rough, causing the darkening observed in these regions in Fig. 1(a). Maximum overgrowth and good surface morphology are obtained for the openings over the angle range between 2 and 26° on either side of the [1$\bar{1}$0] openings. The largest ratio of lateral to vertical growth rates is 5.

After each growth run, cross sections of the overgrown layers were prepared by etching the GaAs from an annular ring concentric with the test pattern. Figures 13(a) and 13(b) are scanning electron micrographs showing such cross sections for two layers, with angles of 4° from a [1$\bar{1}$0] opening and 4° from a [$\bar{1}\bar{1}$0] opening, which were grown on the same substrate at 700°C for

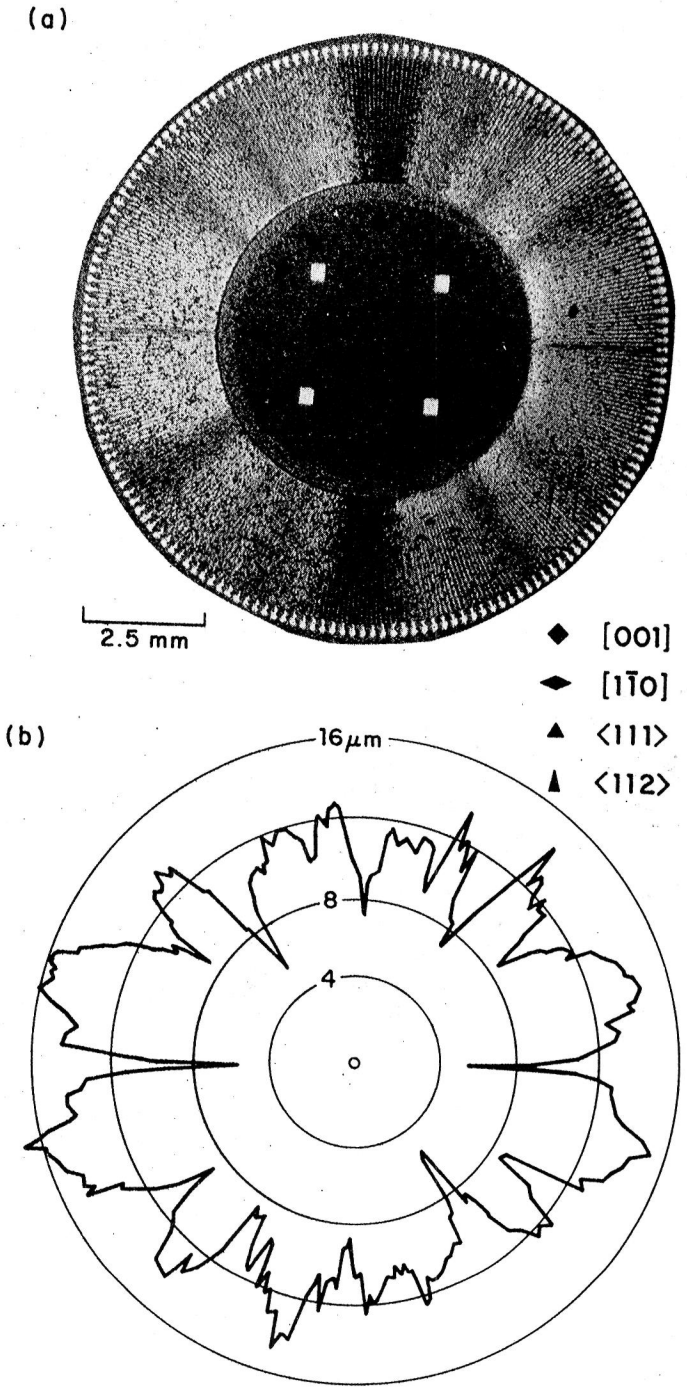

Fig. 12 (a) Photomicrograph of patterned sample after OMCVD growth of GaAs for 18 min at 750°C. Symbols in center indicate low-index directions of lateral growth. (b) Polar plot of layer width vs angle for the sample in (a).

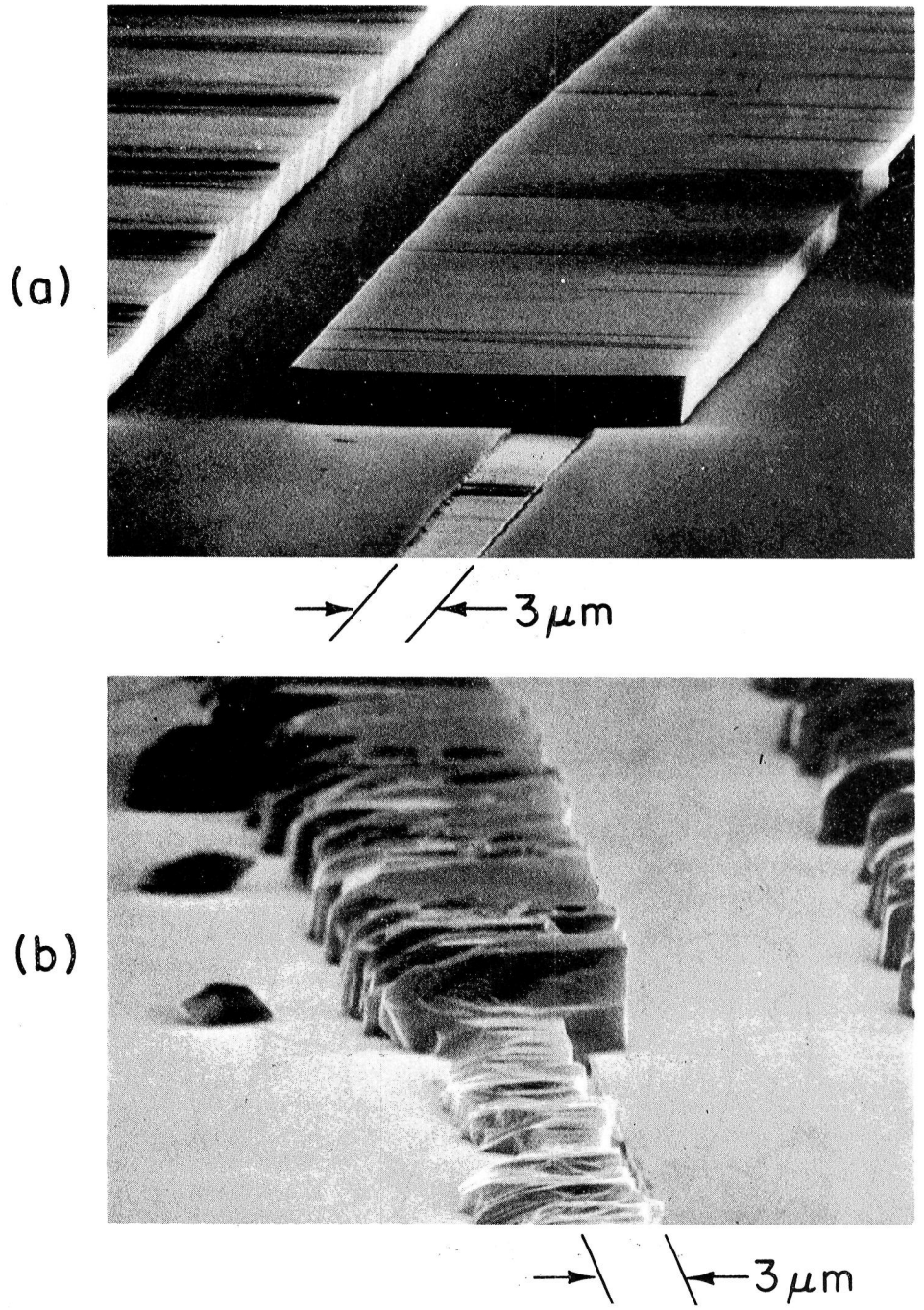

Fig. 13 Secondary electron micrographs, at 87° tilt, showing cross section of GaAs layers with lateral growth directions of (a) 4°clockwise from [110] and (b) 4° counter clockwise from [111]. Layers were grown for 21 min at 700°C.

21 min. The upper area micrograph shows the as-grown surface. In Fig. 13(a) the etch completely removed the GaAs layer from the annular ring, revealing the 3-μm opening in the SiO_2 and the GaAs underneath. The layer in Fig. 13(b) was thicker, however, and some of the layer remained to obscure the opening. Although the two layers had different vertical growth rates, they had the same volume, as given by the product of their height and width. This observation of an orientation independent volume growth rate implies that the volume of material deposited was limited by gas transport in the gas phase, as is generally the case for conventional GaAs OMCVD.[17]

Figure 13 has two other significant features. First, both layers exhibit faceted growth. In vertical OMCVD of GaAs, faceting has been observed due to substrate surface relief[18] or defects in the grown layer.[19] Second, for each layer the lateral growth rates are different on the sides of the stripe opening. These features, as well as the orientation dependence illustrated in Fig. 12, show that the rate of two-dimensional growth by OMCVD is limited by surface kinetics, as well as by mass transport in the gas phase. As in the case of the $AsCl_3$-GaAs-H_2 process, lateral growth by OMCVD is a consequence of the orientation dependence of growth rate associated with surface kinetics. However, there is a significant difference between the two growth processes. In the halide process, there is a dynamic equilibrium between the solid and gas phases, with desorption taking place for a significant fraction of the Ga atoms striking the solid surface. The dependence of the attachment kinetics on orientation makes an important contribution to lateral growth, as well as producing marked differences in the vertical growth rates for different

crystallographic planes. In the OMCVD process, the sticking coefficient for Ga is unity, so that the attachment kinetics are independent of orientation. Once deposited, the Ga atoms can diffuse along the top and side surfaces of the growing layer prior to their incorporation at fixed lattice positions. Lateral overgrowth and faceting in OMCVD result because the diffusing atoms are preferentially incorporated into the different GaAs crystallographic surfaces.

The effect of temperature on lateral growth by OMCVD is shown in Fig. 14, where the total width of the GaAs layer obtained by growth for 15 min is plotted against temperature for the $[1\bar{1}0]$ stripe opening and for two non-$[1\bar{1}0]$ openings. Below 700°C lateral growth decreases because of competition from polycrystalline GaAs deposits that are formed on the SiO_2 film between the openings. These deposits incorporate Ga atoms that are adsorbed on the film and would otherwise diffuse to the growing epitaxial layers. Above 700°C the lateral growth rate for the $[\bar{1}10]$ openings is almost independent of temperature because vertical growth is also taking place in a <110> direction. In this range the rates for the other openings decrease toward the $[1\bar{1}0]$ value, consistent with surface-kinetic-limited growth.

To carry out the CLEFT process, the masking film on the GaAs substrate is patterned with parallel stripe openings at a direction selected for optimum lateral growth. In a growth run, lateral growth takes place until the growth fronts originating from within adjacent openings merge to form a continuous GaAs layer, after which conventional vertical growth continues until the layer reaches the desired thickness. The surface of the layer is then bonded to a

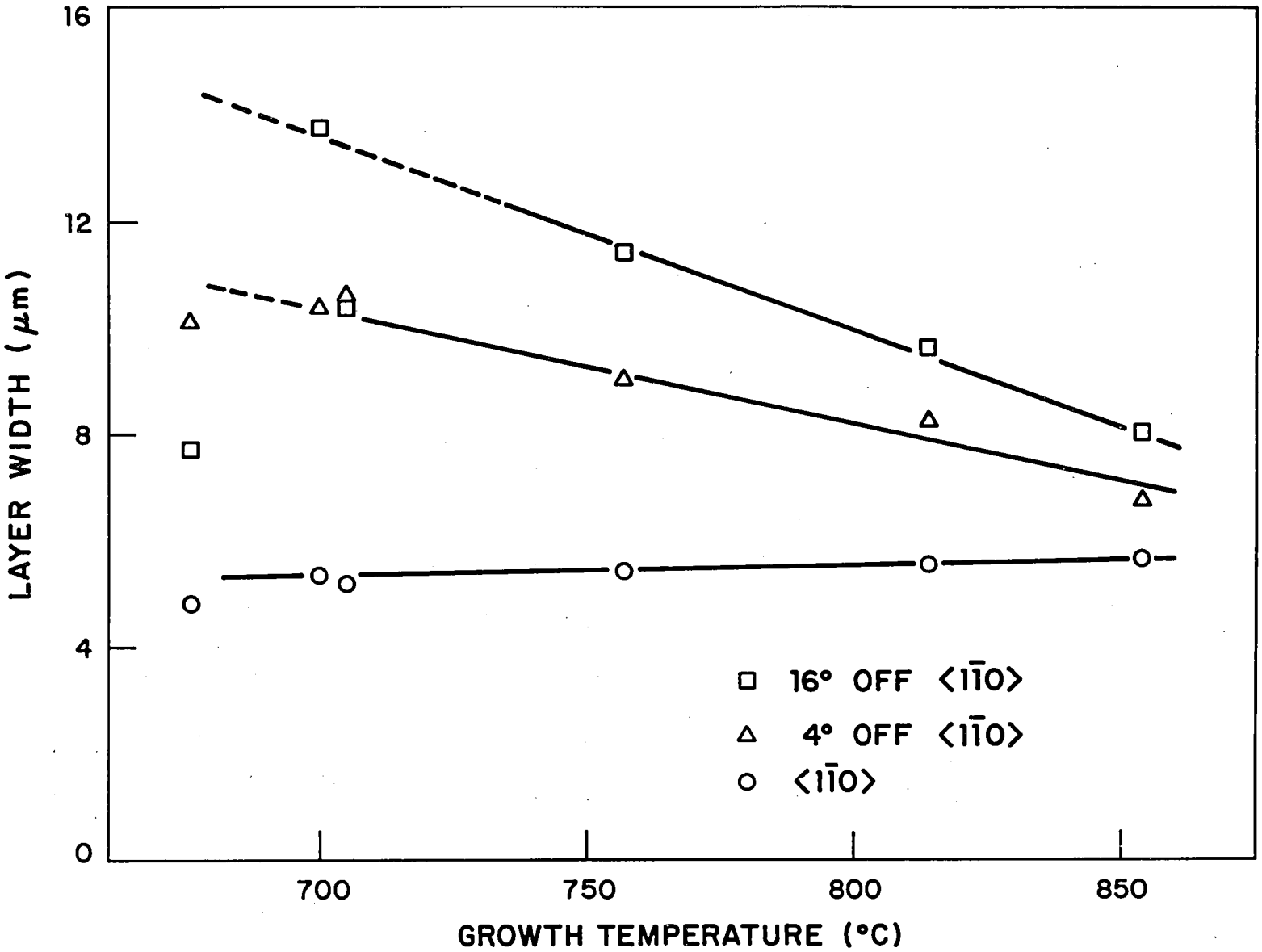

Fig. 14 Width of GaAs layers obtained by growth for 15 min, plotted as a function of growth temperature for three lateral growth directions. For the two non-[110] directions, the dashed lines gives the layer width expected in the absence of GaAs nucleation on the SiO_2.

glass plate or other secondary substrate, and the layer is cleaved from the GaAs substrate. In order to obtain a single-crystal layer, the lateral growth fronts must merge before heterogeneous nucleation of polycrystalline GaAs occurs on the masking film that remains exposed between the stripe openings. In the present study, the rate of such nucleation on SiO_2 was found to decrease with substrate cleanliness, increasing substrate temperature, and decreasing AsH_3/TMGa ratio.

In an initial experiment to demonstrate the applicability of OMCVD to the CLEFT process, we used a substrate mask consisting of successive films of carbonized photoresist and SiO_2 patterned with parallel 4-μm openings, on 10-μm centers, for lateral growth at 20° from $[1\bar{1}0]$. A smooth, continuous epitaxial layer 3-μm thick was obtained by growth at 750°C for 67 min. This layer, which measured 1.0 x 1.6 cm, was bonded to a 250-μm-thick glass substrate and cleaved intact from the GaAs substrate.

IV. SUMMARY

Lateral overgrowth processes have been examined in detail, in $AsCl_3$-GaAs-H_2. The best results have been obtained for (110) substrate orientation, an angle 20° between the slit openings and the cleavage plane perpendicular to the substrate, substrate temperatures somewhat above 700°C, and $AsCl_3$ partial pressure of 4×10^{-3} atm. For sulfur-doped films grown under these conditions, the electron mobility is comparable to that for conventional epitaxial films and TEM studies show that the dislocation density is certainly less than 10^5 cm^{-2} and SCM studies suggest that the dislocation

density is possibly less than 10^3, compared with 10^4 cm^{-2} for the GaAs substrates used. The sulfur concentration is not uniform until the growth fronts from adjacent slit openings join to form a continuous film. The utilization of the CLEFT process in fabricating solar cells has already been demonstrated with efficiencies as high as 17.3% at AM1 for 5.5 μm thick GaAs films.

In OMCVD, we have demonstrated the lateral epitaxial overgrowth of GaAs by OMCVD, and we have established the applicablility of this method to the CLEFT process. Lateral growth, which is due to surface-kinetic control of two-dimensional OMCVD, is a strong function of orientation and growth temperature. On the basis of our observations of lateral growth by OMCVD, the first reported for any material, it apppears very probable that such growth can also be achieved for the other III-V compounds and alloys (e.g., $Ga_{1-x}Al_xAs$ and $GaAs_{1-x}P_x$) that have been prepared by OMCVD. Lateral overgrowth structures incorporating these materials would have important applications in multi-junction solar cells.

REFERENCES

1. J. C. C. Fan, C. O. Bozler and R. L. Chapman, Appl. Phys. Lett. 32, 390 (1978).
2. C. O. Bozler, J. C. C. Fan and R. W. McClelland, Chapter 5 in Gallium Arsenide and Related Compounds (St. Louis) 1978 (The Institute of Physics, London, 1979).
3. J. C. C. Fan, C. O. Bozler and B. J. Palm, Appl. Phys. Lett. 35, 875 (1979).
4. R. W. McClelland, C. O. Bozler and J. C. C. Fan, Appl. Phys. Lett. 37, 560 (1980).
5. C. O. Bozler, R. W. McClelland, J. P. Salerno and J. C. C. Fan, J. Vac. Sci. Technol. 20, 720 (1982).
6. L. Hollan and C. Schiller, J. Cryst. Growth 13/14, 319 (1972).
7. L. Hollan and J. M. Durand, J. Cryst. Growth 46, 665 (1979).
8. L. Hollan, J. M. Durand and R. Cadoret, J. Electrochem. Soc. 124, 135 (1977).
9. J. M. Durand, Philips Res. Rept. 34, 177 (1979).
10. C. O. Bozler, R. W. McClelland and J. C. C. Fan, Electron Device Lett. EDL-2, 203 (1981).
11. M. S. Abrahams and C. J. Buiocchi, J. Appl. Phys. 36, 2855 (1965).
12. J. C. C. Fan, C. O. Bozler, and R. W. McClelland, in Conference Record of the 15th IEEE Photovoltaic Specialists Conference, Orlando, FL, May 1981 (IEEE, New York, 1981) p. 666.

13. R. P. Gale, R. W. McClelland, J. C. C. Fan and C. O. Bozler, Appl. Phys. Lett. 41, 545 (1982).

14. R. D. Dupuis, P. D. Dapkus, R. D. Yinling, and L. A. Moudy, Appl. Phys. Lett. 31, 201 (1977).

15. S. J. Bass, J. Cryst. Growth 31, 172 (1975).

16. J. C. C. Fan, Final Rept "GaAs Shallow-Homojunction Solar Cells," NASA CR-165579, June 30, 1981.

17. P. Balk and E. Veuhoff, J. Cryst. Growth 55, 35 (1981).

18. R. Axoulay, N. Bouadma, J. C. Bouley, and L. Durand, J. Cryst. Growth 55, 229 (1981).

19. R. R. Saxena, C. B. Cooper III, M. J. Ludowise, S. Kikido, V. M. Sardi, and P. G. Borden, J. Cryst. Growth 55, 58 (1981).

DISTRIBUTION

NASA HEADQUARTERS

National Aeronautics and Space Admin.
Technology Utilization Office, Code KT
Washington, DC 20546

National Aeronautics and Space Admin.
Attn: Jerome P. Mullin, Code RTS-6
Washington, DC 20546

National Aeronautics and Space Admin.
Attn: Lynwood Randolph, Code RTS-6
Washington, DC 20546

National Aeronautics and Space Admin.
Scientific and Technical Information Facility
Attn: Accessioning Dept. (30 copies)
P.O. Box 8757
Baltimore/Washington Airport, MD 21240

LEWIS RESEARCH CENTER

NASA-Lewis Research Center
Attn: Dr. Dennis Flood, MS 302-1
21000 Brookpark Rd.
Cleveland, OH 44135

NASA-Lewis Research Center
Attn: Mr. Anthony Long, MS 500-305
21000 Brookpark Road
Cleveland, OH 44135

NASA-Lewis Research Center
Attn: Mr. N. T. Musial, MS 500-318
21000 Brookpark Road
Cleveland, OH 44135

NASA-Lewis Research Center
Attn: Mr. A. F. Forestieri, MS 302-1
21000 Brookpark Road
Cleveland, OH 44135

NASA-Lewis Research Center
Attn: Dr. H. W. Brandhorst, Jr., MS 302-1
21000 Brookpark Road
Cleveland, OH 44135

NASA-Lewis Research Center
Attn: Dr. I. Weinberg, MS 302-1
21000 Brookpark Road (20 copies)
Cleveland, OH 44135

NASA-Lewis Research Center
Attn: Library, MS 60-3
21000 Brookpark Rd. (2 copies)
Cleveland, OH 44135

NASA-Lewis Research Center
Attn: Report Control Office, MS 5-5
21000 Brookpark Road
Cleveland, OH 44135

MARSHALL SPACE FLIGHT CENTER

NASA Marshall Space Flight Center
Attn: Mr. J. L. Miller, Code EC-12
Huntsville, AL 35812

LANGLEY RESEARCH CENTER

NASA-Langley Research Center
Attn: Mr. Gilbert H. Walker, MS 231A
Hampton, VA 23665

NASA-Langley Research Center
Attn: Dr. Edmund Conway, MS 160
Hampton, VA 23665

LYNDON B. JOHNSON SPACE CENTER

NASA-Lyndon B. Johnson Space Center
Attn: Dr. Frank Baiamonte, Code EP5
Houston, TX 77058

NASA-Lyndon B. Johnson Space Center
Attn: Mr. James L. Cioni, Code EP5
Houston, TX 77058

GODDARD SPACE FLIGHT CENTER

NASA-Goddard Space Flight Center
Attn: Mr. Luther W. Slifer, Jr., Code 761
Greenbelt, MD 20771

NAVY

Mr. R. L. Statler, Code 6603F
Naval Research Laboratory
Washington, DC 20390

AIR FORCE

Mr. Joseph Wise,
AFAPL/POE-2
Wright-Patterson Air Force Base, OH
45433

Mr. E. E. Bailey
NASA Technical Liaison
AFAPL/DO
Wright-Patterson Air Foce Base, OH
45433

Dr. Patrick Rahilly
AFAPL/POE-2
Wright-Patterson Air Foce Base, OH
45433

SAMSO SAFSP-8
P.O. Box 92960
Worldway Postal Center
Los Angeles, CA 90009

JET PROPULSION LABORATORY

Dr. Richard Stirn
Jet Propulsion Laboratory
4800 Oak Grove Drive
Pasadena, CA 91103

Dr. Bruce Anspaugh, MS 198-220
Jet Propulsion Laboratory
4800 Oak Grove Drive
Pasadena, CA 91103

Mr. Walter A. Hasbach, MS 198-220
Jet Propulsion Laboratory
4800 Oak Grove Drive
Pasadena, CA 91103

PRIVATE ORGANIZATIONS

Dr. Kim Mitchell
Solar Energy Research Institute
1617 Cole Boulevard
Golden, CO 80401

Mr. John Benner
Solar Energy Research Institute
1617 Cole Boulevard
Golden, CO 80401

Dr. James S. Harris
Rockwell International
Electronics Research Center
P.O. Box 1085
Thousand Oaks, CA 91360

Mr. R. L. Bell
Varian Associates
611 Hansen Way
Palo Alto, CA 94304

Mr. George Wolff
Hughes Aircraft Co.
P.O. Box 92919
Los Angeles, CA 90009

Dr. Sanjiv Kamath
Hughes Research Laboratories
3011 Malibu Canyon Road
Malibu, CA 90265

Dr. Lan Hsu
Space Division, MS SL-10
Rockwell International
12214 Lakewood Boulevard
Downey, CA 90241

Dr. Harold J. Hovel
IBM Corporation Research Laboratories
P.O. Box 218
Yorktown Heights, NY 10598

Dr. James A. Hutchby
Research Triangle Institute
P.O. Box 12194
Research Triangle Park, NC 27709

LANGLEY RESEARCH CENTER
3 1176 00512 1521